University of Groningen

Assessment of the validity of intermolecular potential models used in molecular dynamics simulations by extended x-ray absorption fine structure spectroscopy

Roccatano, D.; Berendsen, H. J. C.; D'Angelo, P.

IMPORTANT NOTE: You are advised to consult the publisher's version (publisher's PDF) if you wish to cite from it. Please check the document version below.

Document Version
Publisher's PDF, also known as Version of record

Link to publication in University of Groningen/UMCG research database

Assessment of the validity of intermolecular potential models used in molecular dynamics simulations by extended x-ray absorption fine structure spectroscopy: A case study of Sr^{2+} in methanol solution

D. Roccatano, H. J. C. Berendsen, and P. D'Angelo

Articles you may be interested in

Comparison of simple potential functions for simulating liquid water
The Journal of Chemical Physics **79**, 926 (1983); 10.1063/1.445869

Particle mesh Ewald: An $N \cdot \log(N)$ method for Ewald sums in large systems
The Journal of Chemical Physics **98**, 10089 (1993); 10.1063/1.464397

A general purpose model for the condensed phases of water: TIP4P/2005
The Journal of Chemical Physics **123**, 234505 (2005); 10.1063/1.2121687

Canonical sampling through velocity rescaling
The Journal of Chemical Physics **126**, 014101 (2007); 10.1063/1.2408420

Polymorphic transitions in single crystals: A new molecular dynamics method
Journal of Applied Physics **52**, 7182 (1981); 10.1063/1.328693

Assessment of the validity of intermolecular potential models used in molecular dynamics simulations by extended x-ray absorption fine structure spectroscopy: A case study of Sr²⁺ in methanol solution

D. Roccatano and H. J. C. Berendsen

Groningen Biomolecular Sciences and Biotechnology Institute (GBB), Department of Biophysical Chemistry, University of Groningen Nijenborgh 4, 9747 AG Groningen, The Netherlands

P. D'Angelo[a]

Dipartimento di Chimica, Università di Roma "La Sapienza," P. le A. Moro 5, 00185 Rome, Italy

Molecular dynamics simulations have been carried out for Sr^{2+} in methanol using different Sr^{2+} Lennard-Jones parameters and methanol models. X-ray absorption fine structure (EXAFS) spectroscopy has been employed to assess the reliability of the ion-ion and ion-methanol potential functions used in the simulations. Radial distribution functions of Sr^{2+} in methanol have been calculated for each simulation and compared with the EXAFS experimental data. This procedure has allowed the determinations of reliable Sr^{2+}-methanol models which have been used in longer simulations providing an accurate description of the dynamic and structural properties of this system. © *1998 American Institute of Physics.* [S0021-9606(98)50622-8]

I. INTRODUCTION

Molecular dynamics (MD) is a powerful tool in the analysis of the chemical and physical properties of molecular systems. This technique has been used to study disordered systems and has contributed to the fuller characterization of their structure.[1] The parameters describing the atomic interaction functions used in MD calculations are usually derived from experimental methods and the validity of the MD results can be assessed by comparison with experimental data.

In recent years, radial distribution functions $g(r)$ obtained from MD simulations have been used as models in the interpretation of EXAFS experimental data.[2–7] This combined approach has produced good results and can thus be used to test the interaction functions employed in the simulations. Comparison of short-range pair distribution functions derived by EXAFS and results of the MD simulations provides a strict test of the reliability and accuracy of the theoretical models used in the simulations. Application of EXAFS is particularly interesting for simple systems, such as ions in solutions. In this case the small number of interaction functions required in the simulations allows each function to be checked and modified on the basis of the EXAFS experimental data, if necessary.

Among the nonaqueous solvents, methanol possesses interesting characteristics as it has both hydrophobic and hydrophilic groups. Methanol molecules form strong hydrogen bonding networks which are responsible for many of the properties of bulk solvent. A large amount of research work has focused on methanol models, but MD studies of ions in methanol are restricted to alkali metal cations[8,9] and to the Mg^{2+} ion.[10] On the contrary, several MD simulations have

been devoted to the study of group I and II cations in aqueous solutions. The Sr^{2+} ion has been extensively investigated in aqueous solutions[7,11–13] and several interaction function parameters (IFP) have been proposed in the literature for the Sr^{2+}-water system while no information is available for the Sr^{2+}-methanol system.

In MD simulations the atomic IFP of a force field are usually optimized using a small set of compounds and their extension to other systems is usually done assuming that they have a low sensitivity with respect to the training set. In the case of alkali ions, IFP optimized for water were used in MD simulations of methanolic solutions.[11] To verify the reliability of this procedure, a comparison of theoretical and experimental values of the solvation free energy was executed.

Here, we present an extensive simulation study of dilute Sr^{2+}- methanol solution with the aim of determining which of the known Sr^{2+} and methanol models provide the most reliable description of the structural properties of the system under investigation. Pair distribution functions of Sr^{2+} in methanol obtained by MD simulations are compared here, for the first time, with experimental results. In particular, different combinations of Sr^{2+} and methanol models have been used to perform MD simulations. Radial distribution functions have been calculated for each simulation and the validity of these models has been assessed on the basis of the EXAFS experimental data. This procedure has allowed the determination of reliable Sr^{2+}-methanol models which have been used in longer MD simulations providing an accurate description of the dynamic and structural properties of this system.

The paper has the following structure. Section II describes the selected interaction function parameters for Sr^{+2} and methanol models. Section III describes the MD procedure and the EXAFS data analysis. In Sec. IV the results of the comparison between the experimental and the MD simu-

lations are described, and the structural and dynamic properties obtained from the MD simulation of the best models are reported and discussed. A summary of the results and the conclusions are given in Sec. V.

II. Sr²⁺ AND METHANOL INTERACTION FUNCTIONS

In previous studies the optimization of the Sr^{2+}-water potential was performed using different approaches. The CHARMM22 (Ref. 14) force field was used by Obst and Bradaczek[12] in the study of the hydration shell of alkaline and alkaline-earth metal cations. This force field contains Sr^{2+} IFP which were tested by comparing calculated static and dynamic properties of Sr^{2+} water solutions with experimental results.

A method for generating EXAFS spectra directly from MD trajectories was recently used by Palmer et al.[7] to investigate strontium chloride aqueous solutions at different temperatures. The Sr^{2+} parameters were provided by private communication. The $g(r)$'s obtained from these simulations were compared with the EXAFS experimental data.

Åqvist optimized the Lennard-Jones (LJ) parameters for Sr^{2+} in water to reproduce the experimental hydration free energy and the radial distribution function derived from x-ray diffraction measurements.[11] The optimization was performed using the simple point-charge (SPC) water model.[15] Use of the SPC water optimized Åqvist parameters for the alkali cations and the methanol solvent model present in the GROMOS87 library[16] was previously shown to be a reasonable approximation and gives good agreement with the experimental data of methanol solutions.[17] In particular, the calculated free energy obtained from this methanol model agrees with the experimental data.

Finally, Spohr et al.[13] performed an *ab initio* calculation of Sr^{2+}-water clusters and the calculated energy points were fitted with an analytical interaction function with three adjustable parameters after the coulombic contributions had been subtracted from the interaction energies. The central force model was employed for water.[18]

In this study we have considered the first three Sr^{2+} LJ parameter sets (namely CHARMM22, Palmer and Åqvist) as they are based on the same type of interaction functions and they have been parameterized to be used with similar water models. The Spohr Sr^{2+} model uses a different type of interaction function which has been parameterized on a different solvent model using a quantum mechanical approach. Therefore, it is too specific to be extended to the methanol models used in our calculations.

Different methanol models have been reported in the literature[19–22] and have been compared to analyze their differences and their capabilities to reproduce the experimental thermodynamic and dynamic properties of pure methanol. The OPLS (Optimized Model for Liquid Simulation)[20,21] and HFM1 (Haughney, Ferrario and McDonald)[19] models were optimized to reproduce the thermodynamic and dynamic properties of liquid methanol, respectively.[19,22] Recently, the OM2 (Optimized Model 2) model was proposed[22] and was shown to produce results comparable to the OPLS and HFM1 models. The geometric parameters of these rigid three

TABLE I. Structural parameters for the GROMOS, OM2, OPLS and HFM1 methanol models. r_{OH} and r_{CO} are the oxygen-hydroxyl hydrogen and the carbon-oxygen distances, respectively.

	r_{OH} (Å)	r_{CO} (Å)	$\widehat{COH}$ (degree)
GROMOS	1.000	1.430	109.47
OM2	1.033	1.425	108.53
OPLS	0.945	1.430	108.50
HFM1	0.945	1.425	108.53

center models are reported in Table I. The LJ parameters and charges used for the different Sr^{2+} and methanol models are summarized in Table II.

In this work we have performed MD simulations assuming complete transferability of the Sr^{2+} IFP optimized for water to methanol models.

III. METHODS

A. Molecular dynamics computational procedure

Twelve simulations have been carried out using all the combinations of the Sr^{2+} and methanol parameters described in the previous section. MD simulations have been performed using an isothermal-isocoric simulation algorithm.[23] The temperature was kept constant at 300 K by weak coupling to an external temperature bath with a coupling constant of 0.1 ps. Simulations were carried out using a rectangular box consisting of one Sr^{2+} ion and 215 methanol molecules subjected to periodic boundary conditions. The box dimensions were chosen to reproduce the density of the liquid methanol. All the MD runs were performed using the program package GROMACS.[24] The SHAKE algorithm[25] was used to constrain bond lengths of the methanol models. A dielectric permittivity, $\epsilon = 1$, and a time step of 2 fs were

TABLE II. LJ parameters and charges used for the simulated atomic species.

	σ_{ii} (Å)	ϵ_{ii} (kJ mol⁻¹)	q_i (u.e.)
CH₃[a]	3.786	0.753	0.150
CH₃[b]	3.775	0.866	0.290
CH₃[c]	3.552	1.104	0.265
CH₃[d]	3.861	0.758	0.297
O[a]	2.955	0.849	−0.548
O[b]	3.071	0.711	−0.690
O[c]	3.220	0.507	−0.700
O[d]	3.083	0.731	−0.728
H[a]	0.0	0.0	0.398
H[b]	0.0	0.0	0.400
H[c]	0.0	0.0	0.435
H[d]	0.0	0.0	0.431
Sr²⁺[e]	3.103	0.494	2.0
Sr²⁺[f]	3.314	0.481	2.0
Sr²⁺[g]	3.523	0.719	2.0

[a]GROMOS.
[b]OM2.
[c]OPLS.
[d]HFM1.
[e]Åqvist.
[f]Palmer.
[g]CHARMM22.

TABLE III. First maximum positions of the Sr-O, Sr-H and Sr-C MD $g(r)$'s (R_O, R_H and R_C, respectively) and coordination numbers (N) for the different methanol and Sr^{2+} models. The estimated deviations are 0.01 Å for the peak positions and 0.2 for the coordination numbers. Distances are given in Å.

	Åqvist				Palmer				CHARMM22			
	R_O	R_H	R_C	N	R_O	R_H	R_C	N	R_O	R_H	R_C	N
GROMOS	2.57	3.27	3.57	8.2	2.67	3.37	3.62	8.3	2.82	3.52	3.77	9.0
OM2	2.62	3.27	3.67	8.1	2.67	3.25	3.72	8.4	2.82	3.52	3.92	8.9
OPLS	2.57	3.17	3.67	8.0	2.62	3.22	3.72	8.2	2.75	3.37	3.82	8.9
HFM1	2.57	3.17	3.67	8.0	2.62	3.22	3.72	8.2	2.82	3.37	3.82	8.9

used. The cutoff radius for the non-bonded interactions was 9 Å. According to Perera et al.[26] use of the simple truncation method, when applied to simulations with only one ion, produces very similar solvation structures to the ones obtained from simulations that employ more accurate techniques for the calculation of the long range interactions. However, for the estimation of solvation energy appropriate corrections must be made.

All atoms were given an initial velocity obtained from a Maxwellian distribution at the desired initial temperature. After the initial minimization of the system, the MD simulations were performed. The first 20 ps were used for equilibration; they have been followed by 100 ps that were used for analysis. The length of the simulation runs of the models using the Sr^{2+} Åqvist IFP was extended up to 1 ns to improve the statistics. These simulations were supplemented by four simulations of the pure methanol models which were used to calculate the solvation entalphy of the Sr^{2+} ion. Moreover, we performed a 1 ns simulation using the Sr^{2+} Åqvist IFP with the SPC water model to compare some structural and dynamical features of the ion in methanol and water. The trajectories were saved every 25 time steps. The sample variance of the average equilibrium properties was calculated by dividing the data taking run into ten sub-blocks. The computed means from each of these sub-blocks were used to calculate the sample variance as described by Bishop and Frinks.[27]

B. The MD g(r)'s

The Sr^{2+}-methanol radial distribution functions were averaged over 100 ps after the equilibration of each simulation. The error on the peak positions[28] was estimated to be 0.01 Å. The radius of the first solvation shell was defined by the first minimum of the $g(r)$. The coordination number N of the ion was obtained from the relation:

$$N = 4\pi\rho \int_0^{R_{min}} g(r)r^2 dr, \qquad (1)$$

where R_{min} is the first minimum of the $g(r)$ and ρ is the density of the system.[28] The position of the first maxima and the N values for the different simulations are reported in Table III.

Figure 1 shows the Sr-O, Sr-H and Sr-C $g(r)$'s obtained from MD simulations using the Åqvist LJ parameters for Sr^{2+} and the GROMOS, OM2, OPLS, and HFM1 methanol models. The results of Fig. 1 indicate that the radial distri-

bution functions obtained from simulations using the same set of LJ parameters for Sr^{2+} and different methanol models are very similar. Note that the position of the first maxima of the Sr-O $g(r)$'s is practically the same for the same Sr^{2+} LJ parameter set, independent of the methanol model used in the simulations. On the contrary, simulations using different sets of LJ parameters for Sr^{2+} and the same methanol model produce radial distribution functions which show more evident deviations in the position of the first maxima. The Sr-O, Sr-H and Sr-C $g(r)$'s obtained from three simulations using the OPLS methanol model and different Sr^{2+} IFP are reported in Fig. 2, as an example. Note that the shifts of the Sr-O first maxima are in the range 0.1−0.25 Å for simulations using different Sr^{2+} LJ parameters and in the range 0.02−0.07 Å for simulations using different methanol models. The number of methanol molecules in the first solvation shell has been found to be different for simulations using different Sr^{2+} LJ parameters. The Sr-O nearest-neighbor distances are very similar to those found from simulations of Sr^{2+} aqueous solutions performed with the same set of IFP.[7,11−13]

As previously noticed for the Mg^{2+} ion in methanol,[10] the Sr^{2+}-methanol $g(r)$'s show very sharp and well defined first peaks. The sharpness of the peaks indicates the presence
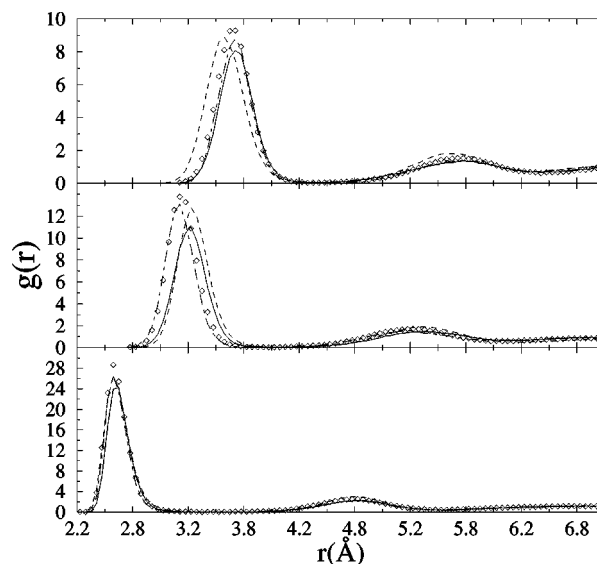

FIG. 1. Sr-O (lower panel), Sr-H (middle panel) and Sr-C (upper panel) pair distribution functions as derived from MD simulations using the GROMOS (dashed line), OM2 (solid line), OPLS (diamonds) and HFM1 (dot-dashed line) methanol models and the Åqvist Sr^{2+} IFP.
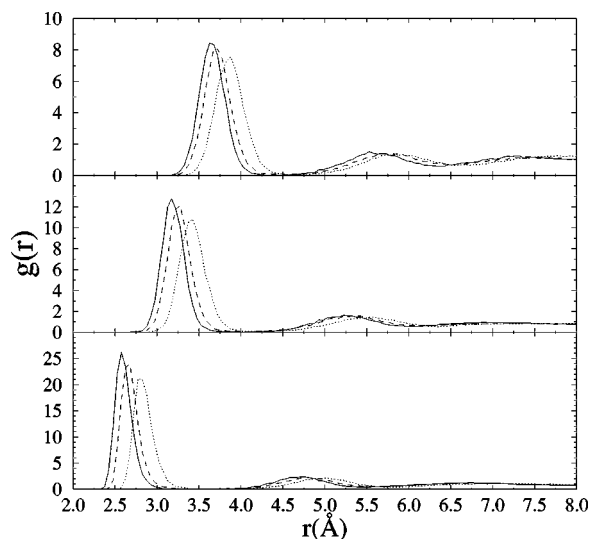
FIG. 2. Sr-O (lower panel), Sr-H (middle panel) and Sr-C (upper panel) pair distribution functions as derived from MD simulations using the Åqvist (solid line), CHARMM22 (dotted line) and Palmer (dashed line) Sr^{2+} IFP and the OPLS methanol model.

of a well organized and defined first solvation shell. The number of methanol molecules in the second solvation shell, which is not accessible by experiments, may be estimated reliably from the simulations. The second solvation shell contains about twice the number of molecules of the first shell. The MD simulation of Sr^{2+} aqueous solutions performed with the Åqvist model in SPC water shows a more populated second shell (≈ 29 water molecules), indicating a tendency of the water molecules to pack more tightly. This is most probably due to the fact that on the average only one hydrogen bond per methanol molecule can be formed between the first and the second solvation shell, while for water about two hydrogen bonds per molecule can be expected.

The methanol-methanol partial $g(r)$'s are very similar to the ones of pure methanol in all the simulations.

C. EXAFS data analysis

A 0.1 M Sr^{2+} methanol solution was obtained by dissolving strontium trifluoro methanesulfonate, prepared as described in Ref. 29, in methanol.

EXAFS spectra at the Sr K edge were recorded in transmission mode using the EMBL spectrometer at HASYLAB.[30] Measurements were performed at room temperature with a Si(220) double-crystal monochromator.[31] Three spectra were recorded and averaged after performing an absolute energy calibration.[32] The DORIS III storage ring was running at an energy of 4.4 GeV with positron currents between 70 and 40 mA. The solution was kept in a cell with a Teflon spacer and Kapton film windows. The spacer thickness was 7 mm.

The EXAFS data analysis is based on a fitting procedure that optimizes the agreement between a model absorption signal α_{mod} and the experimental data α_{exp}.[33] The model signal, as a function of the photon energy E, is given by the relation:

$$\alpha_{mod}(E) = j\sigma_0(E) - [1 + S_0^2\chi(E - E_0)] + \beta(E), \quad (2)$$

where σ_0 is the atomic cross section, j is a scaling factor which accounts for the actual density of the photo-absorber atoms, $\chi(E - E_0)$ is the EXAFS signal containing the structural information, S_0^2 is an amplitude correction factor and is associated with many-body corrections to the one-electron cross section, E_0 defines the energy scale of the theoretical signal and $\beta(E)$ is the background function which accounts for further absorbing processes. The comparison between α_{mod} and α_{exp} is evaluated by means of a square residual function of the type:

$$\mathscr{R}(\{\lambda\}) = \sum_{i=1}^{\mathscr{N}} \frac{[\alpha_{exp}(E_i) - \alpha_{mod}(E_i; \lambda_1, \lambda_2, \ldots, \lambda_p)]^2}{\sigma_i^2}, \quad (3)$$

where $\mathscr{N}$ is the number of experimental points E_i, $\{\lambda\} = (\lambda_1, \lambda_2, \ldots, \lambda_p)$, are the p parameters to be refined, and σ_i^2 is the variance associated with each experimental point $\alpha_{exp}(E_i)$. If we assume that the experimental signal is only affected by random Gaussian noise with standard deviation σ_i, it is possible to perform a rigid statistical evaluation of the results, following standard statistical procedures for non-linear fitting problems. In most cases σ_i^2 can be directly estimated from the experimental spectrum as shown by previous treatments.[34] In many practical cases a k^m weighting (with $m = 2, 3, \ldots$) results in a good approximation. Using this procedure, a full statistical evaluation of the structural results can be performed taking into account the noise of the experimental data.[35] In particular it is possible to calculate the expected value of the residual function $\mathscr{R}$ and evaluate the quality of the fit.[35]

Recent research has revealed the presence of multielectron excitation effects in the x-ray absorption spectra of several atomic and molecular systems.[36] Multielectron transitions are usually associated with the presence of slope changes and unexpected features in the atomic background. The intensity of these contributions can be roughly estimated to be a few percent of the main one-electron channel, thus competing with typical amplitudes of the structural signal. Therefore, the double-electron excitation background is not properly described by the smooth polynomial spline functions that are generally used to extract the EXAFS structural oscillation. In many recent investigations,[4,6,37] the presence of double-electron excitation channels has been accounted for in the EXAFS data analysis by modeling the $\beta(E)$ function as the sum of a smooth polynomial spline plus step-shaped functions, as described in Ref. 37. The presence of anomalous features associated with the simultaneous excitation of $1s4s$, $1s3d$, and $1s3p$ electrons has been detected in the x-ray absorption spectra of Sr^{2+} aqueous solutions.[4] In the present investigation, multielectron transitions have been properly included in the atomic background and the energy positions and the intensities of these resonances have been found to be equal to those determined for Sr^{2+} in water solution.

X-ray absorption spectroscopy is known to be a suitable technique for studying the short-range structure of disordered and ill-ordered systems. Due to the broad correlation func-
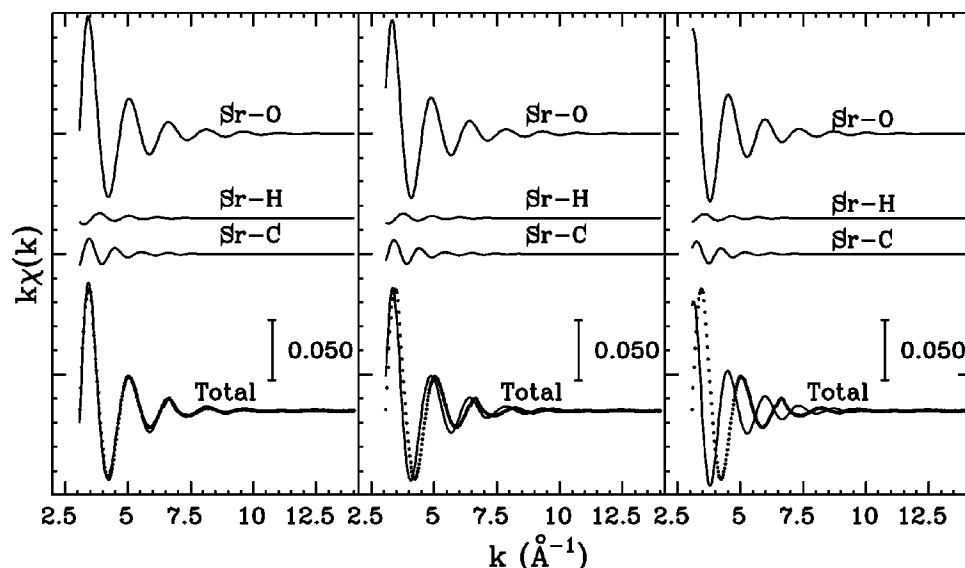
FIG. 3. EXAFS experimental structural signal (dots) of Sr^{2+} in methanol compared with the $\chi(k)$ theoretical signals calculated using the MD $g(r)$'s obtained from the Åqvist, Palmer and CHARMM22 IFP (left, middle and right panels, respectively). From the top to the bottom of each panel the following curves are reported: Sr-O, Sr-H and Sr-C theoretical signals and sum of the previous contributions compared with the experimental data.

tion towards the large distances and to the finite mean-free path of the photoelectron, the sensitivity of EXAFS is limited to the neighborhood (about 5–7 Å) of the photoabsorber atom. Although the experimental characterization of disordered systems over the full range of distances is hampered by this short-range sensitivity, the EXAFS technique has been proved to provide short-distance structural information on disordered systems, which is not possible with other experimental techniques.[2–7]

In the standard EXAFS analysis the coordination of the photoabsorber is usually defined, in the small disorder limit or harmonic approximation, by means of Gaussian shells. This is a valid approximation for solids and liquids in which a high degree of local order is preserved by covalent bonding or strong ion-ion interactions. In general, amorphous and liquid systems are expected to possess moderate to large disorder and the application of this procedure can produce significant errors in the determination of the structural parameters.[38,39] In the case of solutions the radial distribution functions associated with the solvent molecules is asymmetric and the Gaussian approximation is totally inadequate.

A method to analyze EXAFS spectra of liquid systems combining long-range information on the $g(r)$'s obtained from MD simulations, with the short-range sensitivity of the EXAFS, has been described in previous papers.[2] It has been shown that a thorough insight into the interpretation of the EXAFS from liquid matter can be obtained by the calculation of the $\chi(k)$ structural signal associated with different $g(r)$ models. For disordered systems the $\chi(k)$ signal has to be represented by the equation:[40]

$$\chi(k) = \sum_j \int_0^\infty dr 4\pi\rho_j r^2 g_j(r) A_j(k,r)$$
$$\times \sin[2kr + \phi_j(k,r)], \qquad (4)$$

where $g_j(r)$ is the radial distribution function associated with the jth species, $A_j(k,r)$ and $\phi_j(k,r)$ are the amplitude and phase functions, respectively, and ρ_j is the density of the scattering atoms. The high-distance contribution of the $\chi(k)$ signal is damped by the photoelectron mean free path $\lambda(k)$ through an exponential function of the type $\exp[(-r/\lambda(k)]$ which leads to an effective upper integration limit of 5–7 Å in Eq. (4). In our calculations, the photoelectron mean free path, as well as the additional damping factor accounting for the monochromator resolution, is included in the amplitude function $A_j(k,r)$. $\chi(k)$ theoretical signals can be calculated by introducing into Eq. (4) the model $g(r)$'s obtained from MD simulations. Comparison of the theoretical and experimental $\chi(k)$ signals allows the reliability of the $g(r)$'s, and consequently of the models used in the MD simulations, to be checked. Further progress in the understanding of the differences among different MD models can be obtained by applying a peak fitting procedure that refines the short-range shape of the MD $g(r)$'s. Initial asymmetric peaks are obtained by splitting the MD $g(r)$'s into an asymmetric peak and a long-distance tail. In the present investigation the tail contributions to the EXAFS spectrum have been found to be negligible and therefore they have not been considered. As previously described,[2] the asymmetric peaks are modeled with a gammalike distribution function which depends on four parameters, namely the coordination number N, the average distance R, the mean-square variation σ and the skewness β. These parameters are optimized by fitting the EXAFS theoretical signal to the experimental data allowing the refinement of the short-range shape of the MD $g(r)$'s.

The $\chi(k)$ signals associated with the asymmetric peaks have been calculated by means of the GNXAS program.[35,41] Phase shifts and amplitudes have been calculated starting from one of the MD configurations by using muffin-tin potential and advanced models for the exchange-correlation

self-energy (Hedin-Lundqvist).[42] The muffin-tin radii used were 1.59, 0.90, 0.30, and 1.32 Å for the strontium, oxygen, hydrogen and carbon (methyl), respectively. Inelastic losses of the photoelectron in the final state are accounted for intrinsically by complex potential. The imaginary part also includes a constant factor accounting for the core-hole width (3.25 eV).[43]

IV. RESULTS

A. Choice of the Sr^{2+} LJ interaction function

As shown in the previous section MD simulations performed with different methanol models and the same Sr^{2+} LJ parameters produced only slight differences in the shape and position of the Sr^{2+}-methanol radial distribution functions. For this reason the selection of the most reliable Sr^{2+} LJ IFP on the basis of the EXAFS experimental data, has been carried out using the OPLS methanol model as a reference. $\chi(k)$ theoretical signals have been calculated by means of Eq. (4) starting from the MD Sr-O, Sr-H and Sr-C $g(r)$'s. An important first test was optimization of the background parameters only, while keeping fixed the structural parameters derived from the MD simulations. In this way the local structure obtained using MD can be directly compared with experimental data and the validity of the LJ parameters used in the simulations can be assessed. Least-squares fits of the experimental data have been performed in the range $k=3.0–15.2$ Å^{-1} using the FITHEO computer program.[35] In Fig. 3 the comparison between the EXAFS experimental signal and the theoretical contributions calculated using the Åqvist, Palmer and CHARMM22 IFP (left, middle, and right panels, respectively) is reported. The first three curves from the top of each panel represent the Sr-O, Sr-H and Sr-C structural signals, respectively. The remainder of the figure shows the total theoretical contributions compared with the experimental data. From Fig. 3 it is evident that the EXAFS structural oscillation is dominated by the Sr-O contribution, while the Sr-H and Sr-C signals are weaker and mainly affect the low-k region of the spectrum. Nevertheless, as previously observed,[4,6] the inclusion of the hydrogen and carbon signals has been found to be essential to properly reproduce the experimental spectra in the low-k region.

In the case of the Åqvist model the overall agreement between the experimental and theoretical signals is very good and a $\mathscr{R}=1.104\times10^{-5}$ has been obtained. This enforces the reliability of the theoretical model potentials used in the MD simulations. However, the residual function is about 4 times the expected value and the refinement of the short-range structure is necessary to explain this small discrepancy. In the case of the Palmer and CHARMM22 models, while the amplitudes of the simulated signals have the right magnitude, their phases are clearly in disagreement with the experiment. $\mathscr{R}$ values of 1.831×10^{-4} and 1.183×10^{-3} have been obtained for the former and latter model, respectively. This discrepancy is mainly associated with the shift of 0.05 and 0.25 Å in the position of the Sr-O $g(r)$'s first maxima with respect to the Åqvist model (see Table III). Note that the zero position of the theoretical energy scale has been fixed at 0.5 eV above the first inflection point of the
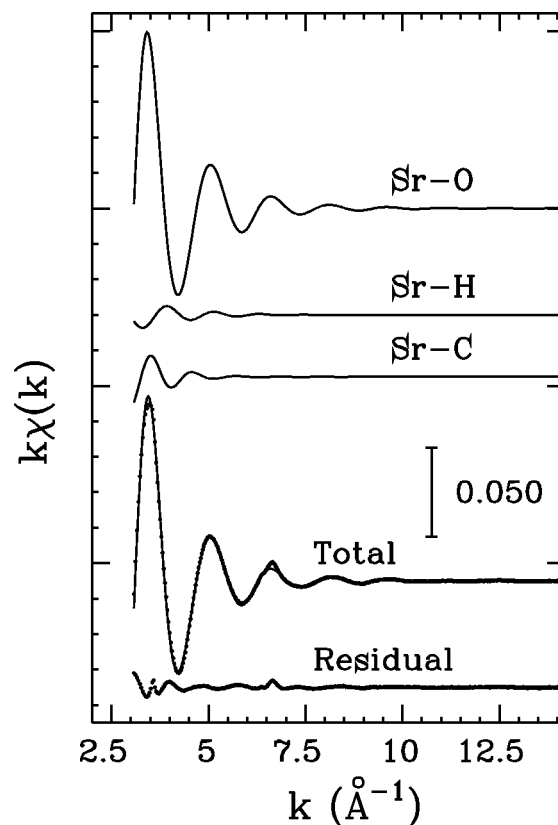

FIG. 4. Best-fit analysis of the Sr^{2+} methanol solution spectrum. From top to bottom the following curves are reported: Sr-O, Sr-H and Sr-C theoretical signals calculated by means of asymmetric peaks, sum of the previous contributions compared with the experimental spectrum and residual.

spectrum in agreement with the analysis of a Sr^{2+} ion in water solution,[4] where the Sr^{2+} first solvation shell is very similar. S_0^2 has been fixed at one.

From the results of this analysis it is clear that the Åqvist potential function provides the best description of the solvent structure around the Sr^{2+} ion. Moreover, comparison with experimental data suggests that the Sr^{2+} Åqvist parameters, which have been designed to reproduce hydration free energies, may be directly transferred to methanol models. Sr-O $g(r)$'s obtained from MD simulations performed with the Palmer and CHARMM22 IFP are shifted towards larger distances with respect to the results of the EXAFS analysis. This indicates that the short-range parts of the Palmer and CHARMM22 interatomic potentials are not able to represent correctly the Sr^{2+}-methanol first solvation shell. It is important to stress that use of different methanol models produced similar results. Moreover, as will be shown in the next paragraph, simulations performed with the OPLS methanol model gave the best agreement with the EXAFS experimental data. In the following sections the Åqvist Sr^{2+} IFP have been used for all further simulations.

B. Analysis of the methanol models

As previously outlined Sr-O $g(r)$'s obtained from MD simulations using different methanol models present very similar features. On the contrary, larger shifts are visible in the maximum positions of the Sr-H and Sr-C $g(r)$'s (see Fig.

TABLE IV. Structural parameters of the Sr-O and Sr-H and Sr-C asymmetric peaks obtained from the EXAFS analysis: R represents the average distance, σ^2 represents the vibrational variance, β is the asymmetry parameter, and N is the coordination number. The standard deviations are in parentheses.

	R (Å)	σ^2 (Å^2)	β	N
Sr-O	2.611(0.003)	0.014 (0.001)	0.3(0.1)	7.2(0.3)
Sr-H	3.16(0.03)	0.023(0.005)	0.5(0.1)	8(1)
Sr-C	3.65(0.03)	0.045(0.004)	0.4(0.1)	7.4(0.8)

1). Comparison of the MD results with the EXAFS experimental data allows the reliability of the different methanol models to be assessed in an objective manner. Furthermore, reliable refinement of the nearest-neighbor peak of the $g(r)$'s can be attempted using the high sensitivity of the EXAFS technique to the short-range structure.

In the first stage of the analysis, comparison with the EXAFS experimental data have been performed fixing the structural parameters to those derived from the MD simulations performed with the four different methanol models. The $\mathscr{R}$ factors for the OPLS, HFM1, OM2, and GROMOS models were 1.104×10^{-5}, 1.484×10^{-5}, 4.545×10^{-5}, and 5.193×10^{-5}, respectively. Also in this case E_0 was fixed at 0.5 eV above the first inflection point of the spectrum and S_0^2 was fixed at one. This direct comparison between MD and EXAFS results shows that the OPLS and the HFM1 models give the best agreement with the experimental data. Nevertheless, the difference in the $\mathscr{R}$ factors between the different models is very small.

Further progress in the determination of the short-range properties of the Sr^{2+}-methanol system has been obtained by applying a peak fitting procedure that refines the short-range shape of the MD $g(r)$'s. As previously outlined, refinement of the first-neighbor distribution requires the optimization of four parameters, R, σ^2, β, and N for each peak of the Sr^{2+}-methanol radial distribution functions. The best-fit analysis of the EXAFS spectrum performed in the range $k = 3.0$–15.2 Å^{-1} is reported in Fig. 4. The first three curves at the top of the figure correspond to the Sr-O, Sr-H and Sr-C theoretical signals calculated from the refined asymmetric peaks. The remainder of the figure shows the total theoretical

FIG. 5. Sr-O, Sr-H and Sr-C asymmetric peaks of Sr^{2+} in methanol (left, middle and right panels, respectively) compared with the MD $g(r)$'s obtained from simulations using the GROMOS (dashed line), OM2 (solid line), OPLS (diamonds) and HFM1 (dot-dashed line) methanol models and the Åqvist Sr^{2+} IFP. Error bars on the asymmetric peaks have been computed starting from statistical errors on individual parameters of Table IV.

contribution compared with the experimental spectrum and the resulting residual. The overall agreement is excellent and the residual function almost coincides with the expected value ($\mathscr{R} = 3.271 \times 10^{-6}$). The accuracy of the data analysis can be appreciated by looking at the residual curve which contains experimental noise, only. Refined values for the full set of parameters defining the short-range peaks of the Sr-O, Sr-H and Sr-C $g(r)$'s are listed in Table IV. Statistical errors on structural parameters have been evaluated accounting for correlations among parameters, and are indicated in brackets.[35] Note that the Sr^{2+}-methanol shell distances obtained from MD calculations cannot be directly compared with the values in Table IV. In the present EXAFS analysis the Sr^{2+}-methanol first shell peaks are modeled with asymmetric peaks where R is the average distance and not the modal value of the distribution. The amplitude reduction factor was found to be $S_0^2 = 1$ and the E_0 energy was found to be 0.5 ± 0.2 eV above the first inflection point of the spectrum.

The refined Sr-O, Sr-H and Sr-C $g(r)$ distributions are shown in Fig. 5 (left, middle, and right panels, respectively), and compared with the results of MD simulations performed with the different methanol models. The Sr-O $g(r)$ derived from the EXAFS analysis is in good agreement with the MD simulations performed with the four methanol models. The first-neighbor peak is found to be less asymmetric than predicted by MD, but the maximum position is in very good agreement. The most interesting effect is that the rise of the first peak is found to be less steep and the foot of the distribution is slightly shifted toward shorter distances. Therefore, the repulsive term of the short-range part of the interatomic potentials used in the MD simulations is found to be too hard. The GROMOS methanol model shows the largest deviation from the EXAFS experimental data. A general remark should be made on the discrepancy in the height of the Sr-O first-neighbor peak between the EXAFS and the MD $g(r)$'s. As shown in Fig. 5 the Sr-O MD $g(r)$'s are out of the reported EXAFS statistical error bars and the coordination numbers obtained from the refinement are lower than the MD ones (see Tables III and IV). The same behavior was observed in previous simulations of Sr^{2+}, Ba^{2+} and Rb^+ in water.[4–6] According to Galera et al.[44] the sharpness of the peaks of the distribution functions obtained from MD simulations is associated with the repulsive r^{-12} term of the LJ potential used to describe the ion-oxygen interaction. This term is commonly used to increase the computational efficiency but an exponential law is a more correct model in the description of the repulsion between the nuclei, according to quantum mechanical considerations.[45] Another approximation used in our MD models which could be responsible for the difference in the coordination number, is the neglect of the polarization effect. As reported in a study of the lanthanide ions in solution,[46] a better description of the structural properties of the simulated ionic solutions can be obtained taking into account the polarizability of the solvent. Note that in the case of the first coordination shell, the high positive charge of the divalent cation can induce large variations in the charge distribution on the solvent molecules altering both the ion-solvent and the solvent-solvent interactions. Therefore it is expected that the induced dipole
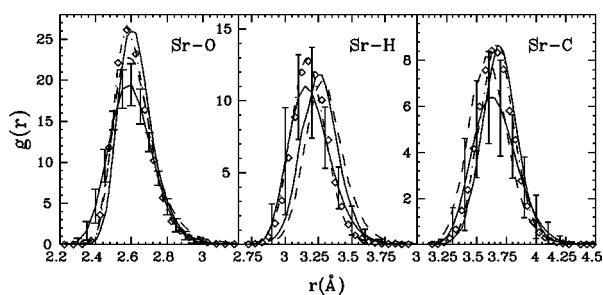
TABLE V. Potential energies (in kJ mol^{-1}) and solvation enthalpies (in kJ mol^{-1}) evaluated from the simulations and standard deviations. E_{MX} is the Sr^{2+}-methanol interaction energy, E_{MM} is the solvent-solvent interaction energy and E_{MM}^p is the pure methanol energy.

	E_{MX}	E_{MM}	E_{MM}^p	ΔH_{sol}
GROMOS	-1628 ± 3	-6766 ± 9	-7320 ± 3	-1339 ± 15
OM2	-2030 ± 2	-7040 ± 6	-7615 ± 6	-1719 ± 14
OPLS	-2002 ± 2	-6792 ± 10	-7560 ± 4	-1497 ± 16
HFM1	-2074 ± 2	-6550 ± 4	-7412 ± 3	-1511 ± 9

interactions between the molecules in the first solvation shell reduce their packing capability.

The first peaks of the Sr-H and Sr-C distributions are determined by EXAFS with large statistical uncertainty. In the case of the Sr-H $g(r)$'s, the curve derived from MD simulations performed with the OPLS and HFM1 methanol models are inside the error bars, while the distributions obtained from the OM2 and GROMOS models are shifted toward larger distances (see Fig. 5). In the case of the Sr-C distributions the $g(r)$ obtained from the OM2 model gives the worst agreement and is shifted towards shorter distance with respect to the experimental determination.

These findings suggest that even if some refinements are necessary for the potential functions of all the methanol models considered, the OPLS and the HFM1 models give the best agreement with the experimental data. Nevertheless, it is important to stress that as the EXAFS $\chi(k)$ signal is sensitive only to the short-range features, the dominant contribution is usually associated with the first peak of the $g(r)$. This hampers an accurate refinement of the MD Sr-H and Sr-C $g(r)$'s on the basis of the EXAFS experimental data. Therefore, in this case the EXAFS technique provides a strict test mainly of the short-range pairwise interactions of the theoretical model potentials used in the MD calculations.

C. Energetics

The average potential energies of the Sr^{2+}-methanol and methanol-methanol interactions of the solution and of the pure solvent simulations are listed in Table V. The ion-solvent interaction energies of the OM2, OPLS and HFM1 methanol models are very similar. The GROMOS model shows a 20% positive deviation from the other models. The methanol-methanol interaction energies of the solution simulations are lower than the pure methanol values due to the strong ion effect with an increase ranging from 12% for the HFM1 model to 8% for the GROMOS one.

The solvation enthalpies (in kJ/mol) have been calculated according to the relation:[47,44]

$$\Delta H_{sol} = E_{MX} + E_{MM} - E_{MM}^p + 1389.35 \left(\frac{1}{\epsilon} - 1 \right) \frac{z^2}{2R_{cut}}, \quad (5)$$

where E_{MX} is the Sr^{2+}-methanol interaction energy, E_{MM} is the solvent-solvent interaction energy and E_{MM}^p is the pure methanol energy. ϵ is the dielectric constant of liquid methanol ($\epsilon = 32$ at 300 K),[48] R_{cut} is the cut-off radius (in Å) used in the simulations (9 Å) and z is the charge of the ion. The last term in Eq. (5) is the simple Born correction associated
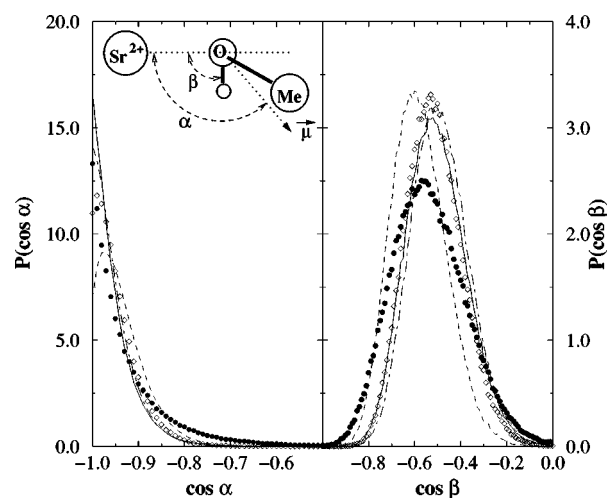

FIG. 6. Distribution of cos α and cos β for the methanol molecules in the first solvation shell of Sr^{2+} obtained from the GROMOS (dashed line), OM2 (solid line), OPLS (diamonds) and HFM1 (dot-dashed line) methanol models compared with the SPC water model distributions (filled circles).

with the cut-off and for methanol it is equal to 299 kJ mol^{-1}. The solvation enthalpies obtained from the simulations are listed in Table V. The experimental value of the solvation enthalpy of Sr^{2+} in methanol has been estimated to be -1506 kJ mol^{-1}. This value has been calculated by adding to the Sr^{2+} hydration enthalpy,[49] the transfer enthalpy of Sr^{2+} from water to methanol.[50] After applying the Born correction the calculated solvation enthalpies of the OPLS and HFM1 models are in good agreement with the experimental value. We note that a further correction due to the neglect of solvent-solvent interactions, which is positive with a magnitude of a few of kJ mol^{-1}, can be applied.[51] In the case of the OM2 and GROMOS models the calculated values are about 15% larger and 11% lower than the experimental determination, respectively. These findings confirm the results obtained from the EXAFS analysis and enforce the OPLS
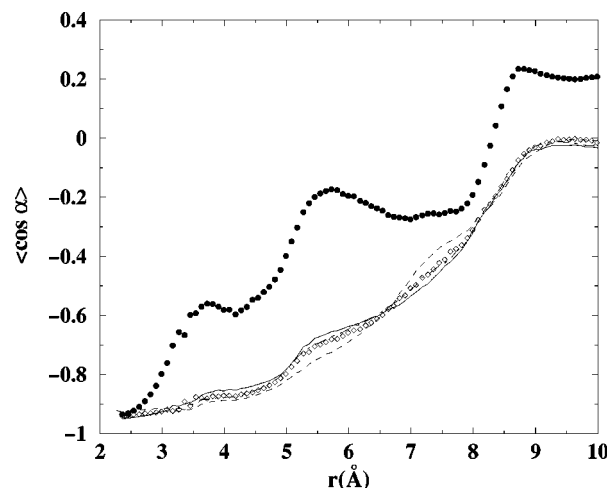

FIG. 7. Average values of cos α for the GROMOS (dashed line), OM2 (solid line), OPLS (diamonds) and HFM1 (dot-dashed line) methanol models as function of the ion-oxygen distance compared with the SPC water model (filled circles).
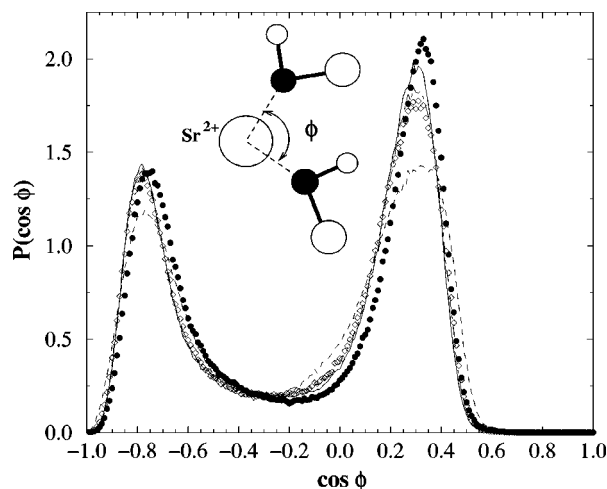
J. Chem. Phys., Vol. 108, No. 22, 8 June 1998

Roccatano, Berendsen, and D'Angelo   9495

FIG. 8. Probability distribution of cos ϕ for the GROMOS (dashed line), OM2 (solid line), OPLS (diamonds) and HFM1 (dot-dashed line) methanol models compared with the SPC water model distribution (filled circles). ϕ is the angle between the Sr^{2+} ion and all the methanol oxygen pairs that belong to the first solvation shell.

and the HFM1 models as the best ones in the description of the structural and dynamic properties of the Sr^{2+}-methanol system.

D. Structure of the first solvation shell

The orientation of the methanol molecules in the first solvation shells is described by the distribution of cos α and cos β. The α and β angles are defined in the inset of Fig. 6. The distribution curves obtained from simulations using the different methanol models are reported in Fig. 6 together with the results of the SPC water simulation. The GROMOS model shows a large deviation in the distribution of cos α and cos β with maxima at $\alpha = 167°$ and $\beta = 107°$. The different distributions of cos α and cos β of the GROMOS model suggest the existence of a different arrangement of the methanol molecules around the Sr^{2+} ion. This is probably due to the fact that the electric dipoles of the GROMOS methanol molecules in the first solvation shell are less aligned to the ion electric field than the methanol molecules of the other models. Moreover, the small difference in the bond angle of the GROMOS model and the low σ value of the CH_3 group of the OPLS model allow a closer packing of the first solvation shell molecules. The SPC water simulation shows a broader distribution due to the higher mobility of the water molecules in the first hydration shell.[13]

In Fig. 7 the average values of cos α are reported as a function of the Sr^{2+}-oxygen distances and compared with the results obtained from the SPC water simulation. Also in this case only slight differences have been found among the OM2, HFM1 and OPLS methanol models while the GROMOS model shows larger deviations. As in the case of Mg^{2+} in methanol,[10] a high degree of order is maintained within 5 Å, beyond which the preferential orientation slowly decreases. In the case of aqueous solution the variations are much larger.

The structure of the solvation shell has been analyzed using the distribution of cos ϕ and the geometrical configu-

TABLE VI. Self-diffusion coefficient (D) in 10^{-5} cm^2/s and residence time in ps. The estimated deviations for the diffusion are 0.1×10^{-5} cm^2/s and for the residence time are about 10%.

	$D_{Sr^{2+}}$	$D_{Solvent}$ (I° shell)	$D_{Solvent}$ (bulk)	τ_N (I° shell)
GROMOS	0.8	1.1	3.5	224
OM2	1.0	1.6	3.7	244
OPLS	0.7	1.0	2.9	262
HFM1	0.7	1.1	2.7	309
SPC	1.1	2.0	5.9	71

ration of the molecules in the shell. The ϕ angle is defined in the inset of Fig. 8. The curves reported in this figure are associated with the four methanol and with the SPC water simulations. The maximum positions obtained from the methanol simulations are almost the same for all the models and are at -0.78 and 0.3, while the curve obtained from the SPC water simulation shows slight differences in the position and height of the two peaks (maximum positions are at -0.75 and 0.33). The first shell is slightly more populated in water than in methanol giving rise to small variations in the packing geometry.

E. Dynamical properties

The self-diffusion coefficients (D) have been calculated from the slope of mean square displacements of the Sr^{2+} ion and of the center of mass of the solvent molecules.[52] In order to study the single ion effect on the translational motions of methanol, the D values have been evaluated separately for two solvent subsystems in the solution, namely the bulk methanol and the Sr^{2+} first solvation shell methanol molecules.[9] To estimate the uncertainty on D the trajectory has been divided into segments of 5 ps and the D values have been calculated for each portion and averaged to give the mean value and its standard deviation.

In Table VI the D values of the three subsystems are reported for the four methanol and for the SPC water models. Using the Nernst-Einstein equation[53] and the limiting molar conductances in methanol of $1/2Sr(ClO_4)_2$ (Ref. 54) and ClO_4^-,[55] an experimental Sr^{2+} self-diffusion coefficient $D_{exp}^{25°} = 0.78 \times 10^{-5}$ cm^2/s has been calculated. This value is very close to the experimental self-diffusion coefficient of Sr^{2+} in water ($D_{exp}^{25°} = 0.79 \times 10^{-5}$ cm^2/s).[48] The self-diffusion coefficient of the Sr^{2+} ion calculated with the SPC water model is smaller than the one calculated by Spohr et al.[13] and is about 28% larger than the experimental value. The self-diffusion coefficient of the Sr^{2+} ion in methanol has been found to be smaller than in water and in agreement with the experimental value. Moreover, it has to be pointed out that the diffusion coefficients of methanol molecules in the bulk are larger than the diffusion coefficients of methanol molecules in the first solvation shell. This finding suggests the formation of a very stable ion-solvent complex. The same behavior has been observed for Mg^{2+} and Na^+ in methanol.[9,10]

Residence times τ_N have been evaluated in terms of maximum and average residence times of solvent molecules in the first solvation shell of the ion. The τ_N values have

been calculated on the basis of the residence time correlation function $R(r,t)$ by using the procedure given by Impey et al.[56] The correlation function $R(r,t)$ measures the number of solvent molecules which initially lie within the first coordination shell and are still there after a time t has elapsed. The characteristic decay time is defined by:

$$\tau_N = \int_0^\infty \langle R(r,t) \rangle dt \qquad (6)$$

since $R(r,t)$ decays exponentially at long times, the characteristic decay time gives a simple definition of τ_N.

The τ_N values for the Sr^{2+} ion in the four methanol models and in the SPC water are reported in Table VI. The large τ_N value of the methanol molecules in the first solvation shell justifies the low value of D. In fact, as explained by the so-called *solventberg* concept,[57] the methanol molecules of the first shell strongly solvate the ion and the resulting complexes migrate together. This leads to an increased effective radius of the ion and to a reduction of its diffusion coefficient.

V. CONCLUSIONS

A detailed investigation of Sr^{2+} in methanol solution has been carried out combining molecular dynamics simulations with EXAFS experimental results. Different Sr^{2+} and methanol models have been combined and simulated and radial distribution functions have been calculated for each simulation. Sr-O, Sr-H and Sr-C $\chi(k)$ signals have been calculated from the MD $g(r)$ models. Comparison of the theoretical and experimental $\chi(k)$ signals has allowed the reliability of the $g(r)$'s, and consequently of the Sr^{2+} and methanol models used in the simulations, to be checked. It was shown that MD simulations performed using the Åqvist Sr^{2+} IFP provide a good description of the solvent structure around the ion. Sr-O $g(r)$'s obtained from simulations performed with the Palmer and CHARMM2 IFP have been found to be shifted towards larger distances with respect to the results of the EXAFS analysis.

Comparison of the MD results with the EXAFS experimental data has allowed the reliability of the different methanol models to be assessed. The short-range sensitivity of the EXAFS technique has been used to refine the nearest-neighbor peaks of the MD $g(r)$'s, providing a strict test of the potential models used in the simulations. The OPLS and HFM1 methanol models have been found to give the best agreement with the EXAFS experimental data, while the GROMOS and OM2 methanol models have shown large deviations in the shape and position of the pair correlation functions.

The solvation enthalpies have been derived from the MD simulations for all the methanol models. The calculated and experimental values are in good agreement in the case of the OPLS and HFM1 models while large deviations have been found in the case of the GROMOS and OM2 models. These findings enforce the results obtained from the EXAFS analysis. Dynamical properties have been analyzed for all the methanol models.

From the results of this investigation it is clear that the EXAFS data are especially well suited to determine the detailed shape of the nearest-neighbor peak in the atom-atom pair correlation functions of disordered systems. The information that they contain about the short-range atom-atom pairwise interactions can be very helpful in specifying and properly modifying the model potential used in MD simulations.

[1] H. Ohtaki and T. Radnai, Chem. Rev. **93**, 1157 (1993).
[2] P. D'Angelo, A. Di Nola, A. Filipponi, N. V. Pavel, and D. Roccatano, J. Chem. Phys. **100**, 985 (1994).
[3] P. D'Angelo, A. Di Nola, E. Giglio, M. Mangoni, and N. V. Pavel, J. Phys. Chem. **92**, 2858 (1995).
[4] P. D'Angelo, H. F. Nolting, and N. V. Pavel, Phys. Rev. A **53**, 798 (1996).
[5] P. D'Angelo, A. Di Nola, M. Mangoni, and N. V. Pavel, J. Phys. Chem. **104**, 1779 (1995).
[6] P. D'Angelo, N. V. Pavel, D. Roccatano, and H. F. Nolting, Phys. Rev. B **54**, 12129 (1996).
[7] B. J. Palmer, D. M. Pfund, and J. L. Fulton, J. Phys. Chem. **100**, 13393 (1996).
[8] D. Marx, K. Heinzinger, G. Pálinkás, and I. Bakó, Z. Naturforsch. Teil A **46**, 887 (1991).
[9] G. Sesé, E. Guàrdia, and J. A. Padró, J. Chem. Phys. **105**, 8826 (1996).
[10] Y. Tamura, E. Spohr, K. Heinzinger, G. Pálinkás, and I. Bakó, Ber. Bunsenges. Phys. Chem. **96**, 147 (1992).
[11] J. Åqvist, J. Phys. Chem. **94**, 8021 (1990).
[12] S. Obst and H. Bradaczek, J. Phys. Chem. **100**, 15677 (1996).
[13] E. Spohr, G. Pálinkás, K. Heinzinger, P. Bopp, and M. M. Probst, J. Phys. Chem. **92**, 6754 (1988).
[14] B. R. Brooks, R. E. Bruccoleri, B. D. Olafson, D. J. States, S. Swaminathan, and M. Karplus, J. Comput. Chem. **4**, 187 (1983).
[15] H. J. C. Berendsen, J. P. M. Postma, W. F. van Gunsteren, and J. Hermans, in *Intermolecular Forces*, edited by B. Pullman (Reidel, Dordrecht, 1981), p. 331.
[16] W. F. van Gunsteren and H. J. C. Berendsen, GROMOS-87 *manual*, Biomos BV, Nijenborgh 4, 9747 AG Groningen, The Netherlands.
[17] J. Åqvist, O. Alvarez, and G. Eisenman, J. Phys. Chem. **96**, 10019 (1992).
[18] F. H. Stillinger and A. J. Rahman, J. Chem. Phys. **68**, 666 (1978).
[19] M. Haughney, M. Ferrario, and I. R. McDonald, J. Phys. Chem. **91**, 4934 (1987).
[20] W. L. Jorgensen, J. Am. Chem. Soc. **103**, 341 (1981).
[21] W. L. Jorgensen, J. Phys. Chem. **90**, 1276 (1986).
[22] P. F. W. Stouten and J. Kroon, J. Mol. Struct. **177**, 467 (1988).
[23] H. J. C. Berendsen, J. P. M. P. W. F. van Gunsteren, A. Di Nola, and J. R. Haak, J. Chem. Phys. **81**, 3684 (1984).
[24] D. van der Spoel, R. van Drunen, and H. J. C. Berendsen, GR*oningen* MA*chine for Chemical Simulations*, Department of Biophysical Chemistry, BIOSON Research Institute, Nijenborgh 4 NL-9717 AG Groningen, 1994.
[25] J. P. Ryckaert, G. Ciccotti, and H. J. C. Berendsen, J. Comput. Phys. **23**, 327 (1977).
[26] L. Perera, U. Essmann, and M. L. Berkowitz, J. Chem. Phys. **102**, 450 (1995).
[27] M. Bishop and S. Frinks, J. Phys. Chem. **87**, 3675 (1987).
[28] M. P. Allen and D. J. Tildesly, *Computer Simulation of Liquids* (Oxford University Press, Oxford, 1989).

[29] G. R. Hedwig and A. J. Parker, J. Am. Chem. Soc. **96**, 6589 (1974).

[30] C. Hermes, E. Gilberg, and M. H. Koch, Nucl. Instrum. Methods Phys. Res. **222**, 207 (1984).

[31] R. F. Pettifer and C. Hermes, J. Phys. Colloq. **C8**, 127 (1986).

[32] R. F. Pettifer and C. Hermes, J. Appl. Crystallogr. **18**, 404 (1985).

[33] E. A. Stern, in *X-Ray Absorption: Principles, Applications, Techniques of EXAFS, SEXAFS and XANES*, edited by D. Koningsberger and R. Prins (Wiley, New York, 1988), Chap. 1.

[34] A. J. Dent, P. C. Stephenson, and G. N. Greaves, Rev. Sci. Instrum. **63**, 8556 (1992).

[35] A. Filipponi and A. D. Cicco, Phys. Rev. B **52**, 15135 (1995).

[36] S. J. Schaphorst, A. F. Kodre, J. Ruscheinski, B. Crasemann, T. Åberg, J. Tulkki, M. H. Chen, Y. Azuma, and G. S. Brown, Phys. Rev. A **47**, 1953 (1993).

[37] P. D'Angelo, A. Di Cicco, A. Filipponi, and N. V. Pavel, Phys. Rev. A **47**, 2055 (1993).

[38] P. Eisenberger and G. S. Brown, Solid State Commun. **29**, 481 (1979).

[39] E. D. Crozier and A. J. Seary, Can. J. Phys. **58**, 1388 (1980).

[40] E. D. Crozier, J. J. Rehr, and R. Ingalls, in *X-Ray Absorption: Principles, Applications, Techniques of EXAFS, SEXAFS and XANES*, edited by D. Koningsberger and R. Prins (Wiley, New York, 1988), Chap. 9.

[41] A. Filipponi, A. D. Cicco, and C. R. Natoli, Phys. Rev. B **52**, 15122 (1995).

[42] L. Hedin and B. I. Lundqvist, J. Phys. C **31**, 1191 (1971).

[43] M. O. Krouse and J. H. Oliver, J. Phys. Chem. Ref. Data **8**, 329 (1979).

[44] S. Galera, J. M. Lluch, A. Oliva, J. Bertrán, F. Foglia, L. Helm, and A. E. Merbach, New J. Chem. **17**, 773 (1993).

[45] J. O. Hirschfelder, C. F. Curtis, and R. Bird, *Molecular Theory of Gases and Liquids* (Wiley, New York, 1954).

[46] T. Kowall, F. Foglia, L. Helm, and A. E. Merbach, J. Phys. Chem. **99**, 13078 (1995).

[47] J. Chandrasekhar, D. C. Spellmeyer, and W. L. Jorgensen, J. Am. Chem. Soc. **106**, 903 (1984).

[48] *CRC Handbook of Chemistry and Physics*, 74th ed., edited by D. R. Lide (Chemical Rubber, Cleveland, 1993–1994).

[49] Y. Marcus, *Ion Solvation* (Wiley, New York, 1985).

[50] M. Chaudhry, Y. Kinjo, and I. Persson, J. Chem. Soc., Faraday Trans. **90**, 2683 (1994).

[51] R. H. Wood, J. Chem. Phys. **103**, 6177 (1995).

[52] J. P. Hansen and I. R. McDonald, *Theory of Simple Liquids* (Academic, London, 1986).

[53] J. O. Bockris, *Modern Electrochemistry* (Plenum, New York, 1970).

[54] H. Doe, K. Wakamiya, and T. Kitagawa, Bull. Chem. Soc. Jpn. **60**, 2231 (1987).

[55] H. Doe and T. Kitagawa, Bull. Chem. Soc. Jpn. **58**, 2975 (1985).

[56] R. W. Impey, M. Sprik, and M. L. Klein, J. Am. Chem. Soc. **109**, 5900 (1987).

[57] S. H. Lee and J. C. Rasaiah, J. Chem. Phys. **101**, 6964 (1994).